

A Ka-band Wavemill Instrument Study for Ocean Surface Velocity Retrieval

5th Workshop on Advanced RF Sensors and Remote Sensing Instruments, ARSI'17 &
3rd Ka-band Earth Observation Radar Missions Workshop, KEO'17

12-14 September 2017

ESA/ESTEC, Noordwijk, The Netherlands

Steffen Wollstadt¹, Marwan Younis¹, Marc Rodriguez-Cassola¹, Sigurd Huber¹,
Paco López-Dekker², Christopher Buck³

¹German Aerospace Center (DLR), Microwaves and Radar Institute, Oberpfaffenhofen, Germany

Email: steffen.wollstadt@dlr.de

²Delft University of Technology, Delft, The Netherlands

³ESA/ESTEC, Noordwijk, The Netherlands

I. INTRODUCTION

During the last years there has been increased focus on the measurement of ocean currents and surface velocities at sub-mesoscale resolutions. In order to obtain 2-D measurements, the investigations and studies have been predominantly based on dual-beam along-track Synthetic Aperture Radar interferometry (DBI/ATI SAR) [1], [2]. Also ESA initiated several studies based on this measurement concept, which resulted in the development of the Wavemill concept [3], [4]. The following ESA Ocean Surface Current Mission Study (OSCMS) has introduced two independent mission and instrument concepts in Ku-band [5], [6]. Since strong scientific requirements on this mission, such as swath coverage and product resolution, result in large instruments, Ka-band technology is a suggested solution in order to reduce the mission size. The objective of this study is the conceptual design of a Wavemill instrument in Ka-band and its comparison to the OSCM instrument in Ku-band. Advantages of each frequency band regarding mainly the sensitivity will be identified, since the required sensitivity determines the size of the instrument.

The instrument design methodology is sensitivity-based and identical to the OSCM design [7]. A detailed description of the OSCM study and the DBI/ATI measuring principle can be found in [6], [7], [8]. In order to compare both systems with respect to the frequency bands, the same requirements have been applied. They are given in Table I. It is worth to mention, that the measured quantity of the instrument is the Doppler velocity of the full sea state, which is not corrected for any other wind contribution. Furthermore the applied methodology accounts only for system errors and does not consider any geophysical or inversion errors. A main difference of the Ka-band concept is the choice of the antenna type, which is reflectarray-based. One of the crucial advantages of investigating a similar concept in Ka-band is the increased sensitivity thanks to the electrically larger interferometric baseline.

Table I. Driving system requirements

Swath coverage	200 km
Surface velocity accuracy	5 cm s ⁻¹
Minimum surface wind (U_{10})	3 m s ⁻¹
Product resolution	4 km
Operating frequency	Ka-band

In Section II the sensitivity and interferometric baseline of Ka- and Ku-band is compared. Section III shows the instrument and antenna concept. In Section IV the SAR and interferometric performance is presented and Section V concludes the paper.

II. SENSITIVITY AND INTERFEROMETRIC BASELINE

The interferometric baseline is a crucial figure in an ATI SAR system. The decision for a baseline implies a trade-off between the physical instrument dimensions and the measurement sensitivity. It basically means that keeping, for example, the 12 m baseline used within the Ku-band system - and everything else being equal - would increase the sensitivity of the Ka-band system by approximately 8 dB. On the contrary, a baseline scaling by the ratio of the wavelengths (factor 2.6) would keep the sensitivity, but decrease the system length to approximately 4.6 m, again, everything else remaining equal. A smaller instrument size means a reduction of mass and costs.

Figure 1 shows the surface current error as a function of the physical baseline for different wind speeds and different signal-to-noise-ratios (SNR). This error accounts for the (random) measurement noise, which cannot be mitigated [7]. It depends on the SNR, the resolution (or number of looks) and the along-track baseline. A 3 cm/s error is denoted by a horizontal line, which indicates approximately the maximum scientifically allowed measurement error magnitude. Depending on the wind speed and SNR the optimum baseline is around 40-50 m ($\approx 2000\lambda$) for the Ku-band case, which is quite large for a single satellite mission. And 12 m length in the OSCM solution is clearly below the optimum, which limits the performance, for example, the product resolution. In Ka-band, on the other hand, the 12 m baseline fits exactly in the optimum baseline range around 20 m ($\approx 2000\lambda$). A scaling of the baseline with the wavelength to 4.6 m will again result in a decrease of performance parameters such as product resolution or swath width.

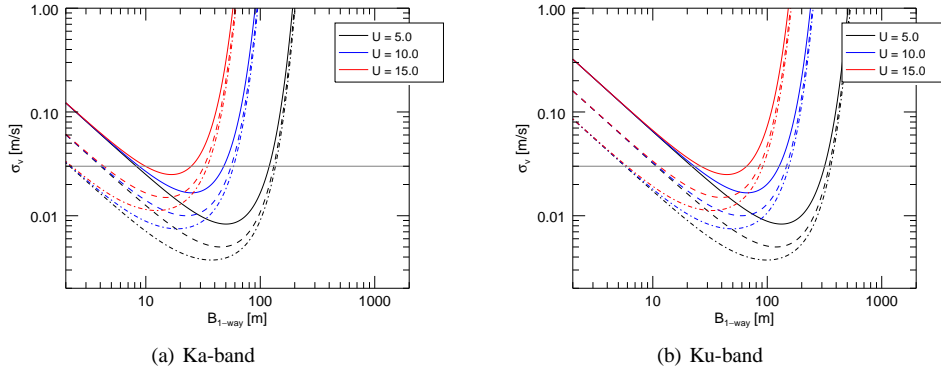


Fig. 1. Surface current velocity standard deviation as a function of the physical baseline for different wind speeds (U) and SNRs of 0 dB (solid), 5 dB (dashed) and 10 dB (dotted/dashed).

However, considering the sensitivity in Ka-band means at the same time to account for contributions which reduce the positive baseline effect. First, the atmospheric losses have to be assumed in the best case with 4 dB (clear sky loss), which is around 3 dB more than in Ku-band. Second, the impact of the antenna size is dependent on several mechanisms. For higher frequency bands a different antenna type such as reflectarray antennas is favorable, which proposes, for example, a rather short antenna length, since the efficiency of a reflectarray antenna is better for circular apertures. The overall sensitivity improvement is unfortunately not straightforward, since it is mutually coupled with the interferometric sensitivity through the resolution. An increase of the antenna length results obviously in a worse resolution, a smaller number of looks, and finally in less interferometric sensitivity, which contradicts the improved antenna gain. But also a decreased antenna length yields a worse resolution when considering the suggested ScanSAR approach. A shorter antenna requires a higher pulse repetition frequency (PRF), narrower sub-swaths and therefore more sub-swaths. In our case the number of sub-swaths increased from 3 to 5 which means a sensitivity decrease of 1.7 dB. Third, also the antenna efficiency is supposed to be lower for a reflectarray antenna, which is assumed with, at least, around 1 dB less. And this does not even account for most likely additional thermal system-losses in Ka-band. And finally fourth, the available transmit (Tx) power has obviously a large impact. Currently high power amplifiers (HPAs) with 3 kW are available in Ka-band [9]. Assuming the use of rather less HPAs in Ka-band due to thermal considerations, a Tx peak power decrease from 10 to 7 kW reduces the sensitivity by another 1.8 dB. In total we end up with a sensitivity decrease of around 7.5 dB, which is the reason for staying with the 12 m baseline. Basically we have to trade the sensitivity provided by the baseline with increased atmospheric losses, the antenna size, and the available Tx power.

III. INSTRUMENT AND ANTENNA CONCEPT

This section presents the instrument and antenna concept including parameters of the operation mode, RF-front end and the acquisition geometry. In general reflectarray antennas with large apertures are highly efficient with low costs and simple manufacturing. The DBI concept requires two simultaneous beams in two different directions, which is, compared to reflector antennas, more easily to achieve with reflectarrays due to the flexible steering capability. A reflectarray system is also supposed to be beneficial compared to a waveguide array antenna with respect to the lossy power distribution in Ka-band. The used antenna concept consists of a basic reflectarray geometry for each antenna, which can be seen in Fig. 2. The antenna beam patterns are calculated by a simple geometric antenna model. The following assumptions and simplifications are made: Array elements are idealized, no antenna element cross-talk is considered, no blockage or multi-path propagation effects is considered and no tapering or beam broadening is applied.

The concept is based on the same canonical Ku-band system presented in [6], except of using reflectarray antenna technology. Fig. 2 shows the concept with two receive (Rx) antennas, separated by a 12 m baseline and an additional, centered transmit (Tx) antenna. This design ensures that the Tx antenna is close to the satellite bus, where the power generation is located. It also avoids the usage of circulators and mitigates (on Rx) losses in distribution networks and losses due to temperature/heat dissipation. Each Rx antenna setup consists of two reflectarray antennas on top of each other. One is looking forward, the other in the aft direction, both with an azimuth squint of 18.5° . A look angle range of 8.6° is necessary to cover the 200 km swath width. Both arrays are printed, dual-polarized microwave patch antennas. The total size is 2.4 m x 3.56 m (2x1.78 m). The (dual-polarized) feeds are located in the center of the antenna with a focal length of 1.56 m. 46 feeds are necessary for each antenna to achieve the swath coverage. The total feed height is $2 \times 0.385 \text{ m} = 0.77 \text{ m}$. In this conceptual approach the Tx antenna is identical to the Rx antenna except for the array height. It is estimated to around 0.2 m. For the illumination of each of the five sub-swaths 10 to 14 active feeds (out of 46 in total) are necessary, where some active feeds are always overlapping with respect to the sub-swaths. Regarding polarization, the Tx feeds transmit circular polarization. Dual polarized feeds have to be applied, which radiate both polarizations with a 90° phase shifted signal and an additional time delay. The circular polarization on Tx and dual-polarized, linear polarization on Rx enable the so-called hybrid polarization.

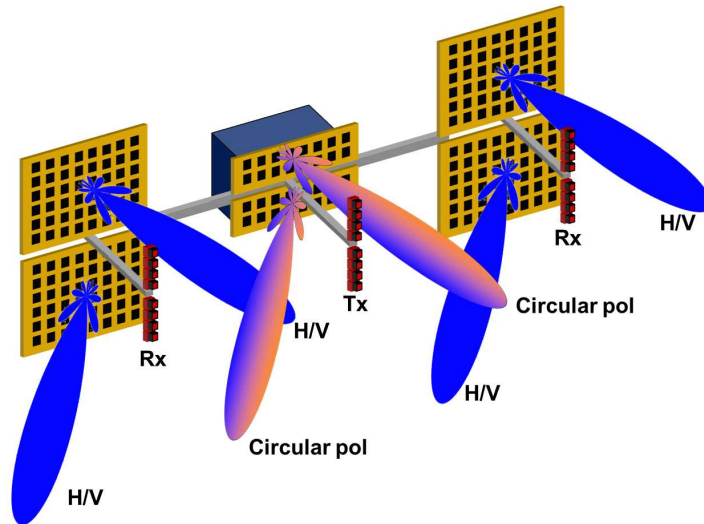


Fig. 2. Canonical DBI/ATI Instrument Concept: 2 Rx & 1 Tx reflectarray antenna set-up

Additional and more detailed parameters about the RF-front end, the operation mode and the acquisition geometry are given in Table II. For implementation of the presented basic design one should consider antenna optimization options such as a secondary reflectarray or a geometry, where the feeds are directly mounted to the satellite bus, in order to improve the power distribution/losses.

IV. PERFORMANCE AND SYSTEMATIC ERRORS

This section presents the SAR performance and the interferometric performance of the system. Only system-based errors are considered, which are the (random/interferometric) measurement errors and the systematic errors. Geophysical and inversion errors are not taken into account. After evaluation of the interferometric performance, a limit

Table II. Main instrument and operating mode parameters.

Acquisition Geometry			
Orbit height	798 km	ATI baseline	12 m
Azimuth squint	$\pm 18.5^\circ$	Antenna tilt	20.1°
Antenna			
Single Transmit Sub-Antenna		Single Receive Sub-Antenna	
Length	2.4 m		2.4 m
Height	0.2 m		1.78 m
Gain	47.5 dB		54.8 dB
Ant. efficiency	0.63		0.63
Losses	0.5 dB		0.5 dB
Polarization	Circular		2 lin. orthog. channels
Average Tx RF power	210 W	Noise temperature	440 K
(Total Avg. Tx RF power)	(840 W)	Atmospheric loss	4 dB
Operating Mode			
SAR mode	ScanSAR	DBF mode	SCORE
Number of bursts	5	Swath coverage	200 km
Pulse duty cycle	12%	Data rate	310.9 Mbit/s
Pulse bandwidth			5/5/5/5 MHz
PRF			6850/6555/6760/6800/7000 kHz
Proc. Doppler bandwidth			168/130/147/255/1306 Hz

for the systematic errors are calculated in order to fulfill the 5 cm/s velocity accuracy. The applied sensitivity-based methodology is described in [7]. In principle, we are interested in the product resolution, which is determined by the 2-D resolution and the number of looks. So we can apply a better geometric resolution (and therefore a higher number of looks) where it is necessary regarding the swath (incident angle range).

Fig. 3 shows the noise-equivalent-sigma-zero (NESZ) and the corresponding SNR and backscatter model. The olive-colored curves in Fig. 3a denote the requirement to fulfill a 3 cm/s surface velocity error. The reason for the dominant, v-shaped trend is a strong defocussing at the outer feeds due to the large dimension of the overall feed. Note that the 1-D azimuth resolution for each swath is [29, 40, 38, 23, 4.5] m, which result in a number of looks of around 10000 for the first four sub-swaths but around 60000 for the last sub-swath. The applied backscatter model is a modified Ku-band model (NSCAT3) with 1 dB higher coefficients (based on the results of [10]).

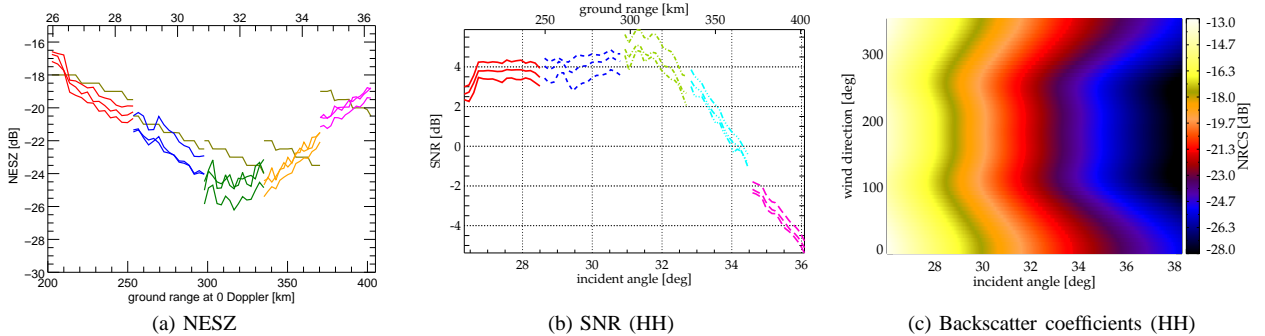


Fig. 3. Sensitivity results: NESZ and corresponding SNR and modified NSCAT3 backscatter model. (The three different lines in (a)/(b) denote three different azimuth positions, which are seen with the center and edges of the beam.)

In Fig. 4a, based on the sensitivity results, the interferometric surface velocity error is shown. Fig. 4b presents the summarized systematic errors. Maximum errors for attitude knowledge, baseline deformation and instrument phase are determined in order to stay below the 5 cm/s accuracy requirement. Here the RSS error for a $1 \mu\text{rad}$ attitude error (in yaw, pitch and roll), including a relative baseline deformation, and 0.55° phase error is given. Of course the error contributions can be distributed differently. Finally Fig. 4c shows the total surface velocity error.

V. SUMMARY AND COMPARISON

The presented Ka-band instrument concept meets the given requirements in Table I, however, it is quite large. The 12 m baseline of the Ku-band concept has to be kept in order to compensate other increased sensitivity requirements

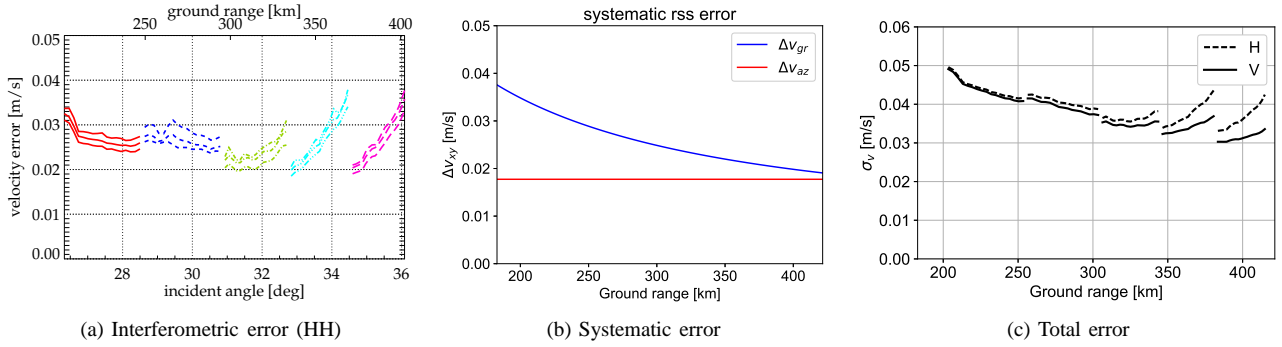


Fig. 4. System-based surface velocity error. (The systematic errors denote a requirement in order to achieve the total error requirement of 5 cm/s.)

regarding atmospheric losses, Tx power and antenna size/type, which is discussed in Section II. In this approach the antenna length of 2.4 m has been chosen as the minimum length, which satisfies the azimuth ambiguity ratio requirement. The available Tx power has been assumed less compared to the Ku-band study. In general the polarimetric DBI/ATI concept implies strong constraints regarding power consumption and antenna geometry/type due to the simultaneous polarimetric fore and aft looking set-up. However, the approach in this study presents the required order of magnitude regarding size and geometry. Further optimizations with respect to antennas and feeds are possible. Furthermore, with the necessary low pulse bandwidth of 5 MHz, the sensitivity requirement is achieved, but one has to keep in mind that, for a surface velocity inversion with the acquired ATI data, ideally the full wave spectrum has to be resolved.

Taking a more global look to the instrument transition from Ku- to Ka-band, it seems that there is only little potential for improvements due to Ka-band. The main driving scientific issues still remain the same and are still of paramount importance: If the wind speed dependency shall be decreased to the desired 2 m/s (which means down to which wind speed the measurement is valid) the required sensitivity increases by 3-4 dB. The required large swath coverage is also demanding, i.e., 50 km swath width in far range mean 2 dB of required sensitivity. But most important and demanding is for sure the desired product resolution. The Ku-band as well as the Ka-band approach assume a product resolution of 4 km in each direction. A decrease to the scientifically required 1 km or less would imply a required sensitivity increase of 12 dB.

VI. ACKNOWLEDGEMENT

This work has been funded by ESA-ESTEC under contract no. 4000111249/14/NL/FE.

VII. REFERENCES

- [1] E. Rodriguez, D. Imel, and B. Houshmand, "Two-dimensional surface currents using vector along-track interferometry," in *Proc. PIERS*, 1995, p. 763.
- [2] S. Frasier and A. Camps, "Dual-beam interferometry for ocean surface current vector mapping," *IEEE Transactions on Geoscience and Remote Sensing*, vol. 39, no. 2, pp. 401–414, Feb. 2001.
- [3] C. Buck, C. Donlon, and N. Gebert, "A Status Update of Investigations into the Wavemill Concept," in *EUSAR 2014; 10th European Conference on Synthetic Aperture Radar; Proceedings Of*, Jun. 2014, pp. 1–4.
- [4] C. Gommenginger, B. Chapron, J. Marquez, B. Richards, M. Caparrini, G. Burbidge, D. Cotton, and A. C. Martin, "Wavemill: A new mission for high-resolution mapping of total ocean surface current vectors," in *EUSAR 2014; 10th European Conference on Synthetic Aperture Radar; Proceedings Of*, Jun. 2014, pp. 1–4.
- [5] S. Doody, J. Marquez, B. Dobke, C. Gommenginger, and A. Martin, "A mission for measuring ocean surface current vectors," in *Proceedings of EUSAR 2016: 11th European Conference on Synthetic Aperture Radar*, Jun. 2016, pp. 1–4.
- [6] S. Wollstadt, P. López-Dekker, F. De Zan, M. Younis, R. E. Danielson, V. Tesmer, and L. Martins-Camelo, "A Ku-band SAR Mission Concept for Ocean Surface Current Measurement using Dual beam ATI and Hybrid Polarization," in *Geoscience and Remote Sensing Symposium (IGARSS), 2015 IEEE International*, Jul. 2015, pp. 1219–1222.

- [7] S. Wollstadt, P. López-Dekker, F. D. Zan, and M. Younis, "Design Principles and Considerations for Spaceborne ATI SAR-Based Observations of Ocean Surface Velocity Vectors," *IEEE Transactions on Geoscience and Remote Sensing*, vol. 55, no. 8, pp. 4500–4519, Aug. 2017.
- [8] P. López-Dekker, F. De Zan, S. Wollstadt, M. Younis, R. E. Danielson, V. Tesmer, and L. Martins-Camelo, "A Ku-Band ATI SAR Mission for Total Ocean Surface Current Vector Retrieval: System Concept and Performance," in *Proc. of Advanced RF Sensors and Remote Sensing Instruments Workshop (ARSI'14)*, ESA-ESTEC, Noordwijk, The Netherlands, Nov. 2014.
- [9] B. Steer, A. Roitman, P. Horoyski, M. Hyttinen, R. Dobbs, and D. Berry, "Advantages of extended Interaction Klystron Technology at Millimeter and Sub-Millimeter Frequencies," in *Proceedings of 16th Pulsed Power Conference*, Albuquerque, Canada, 2007, CPI - Communications & Power Industries Canada Inc., 45 River Drive, Georgetown, Ontario L7G 2J4.
- [10] S. Tanelli, S. L. Durden, and E. Im, "Simultaneous measurements of ku- and ka-band sea surface cross sections by an airborne Radar," *IEEE Geoscience and Remote Sensing Letters*, vol. 3, no. 3, pp. 359–363, Jul. 2006.